



LAWRENCE
LIVERMORE
NATIONAL
LABORATORY

Band-Notched UWB Equiangular Spiral Antenna

J. H. Jeon, J. T. Chang, A. Pham

December 5, 2013

IEEE International Microwave Symposium
Tampa Bay, FL, United States
June 1, 2014 through June 6, 2014

Disclaimer

This document was prepared as an account of work sponsored by an agency of the United States government. Neither the United States government nor Lawrence Livermore National Security, LLC, nor any of their employees makes any warranty, expressed or implied, or assumes any legal liability or responsibility for the accuracy, completeness, or usefulness of any information, apparatus, product, or process disclosed, or represents that its use would not infringe privately owned rights. Reference herein to any specific commercial product, process, or service by trade name, trademark, manufacturer, or otherwise does not necessarily constitute or imply its endorsement, recommendation, or favoring by the United States government or Lawrence Livermore National Security, LLC. The views and opinions of authors expressed herein do not necessarily state or reflect those of the United States government or Lawrence Livermore National Security, LLC, and shall not be used for advertising or product endorsement purposes.

Band-Notched Equiangular Spiral Antenna

Jae H. Jeon, John T. Chang
Lawrence Livermore National Laboratory
Livermore, CA
jeon2@llnl.gov, chang16@llnl.gov

Anh-Vu Pham
Department of Electrical and Computer Engineering
University of California Davis
Davis, CA
pham@ece.ucdavis.edu

Abstract—A band-notched ultra-wideband equiangular spiral antenna is presented. Top layer of the substrate is printed with equiangular spiral geometry. Bottom side is used for a secondary resonant structure to create a notch filter response over the 802.11a band. VSWR of 2:1 is achieved for the FCC UWB band, which is 3.1 to 10.6 GHz. For the notch band, which is 5.15 to 5.85 GHz, VSWR exceeds 2:1, peak rejection reaching 12:1 at the center of the band at 5.5 GHz. Suppression of radiation in this band is evident in its gain profile over frequency and in current density plot around the resonant structure as well. Simple control of two design parameters can readily move the notch band. The proposed antenna is fabricated on a Rogers Duroid substrate along with a custom designed balun. The simulation results are validated through experimental measurements.

Keywords—Band-notched, ultra wideband (UWB), spiral antenna,

I. INTRODUCTION

In general, ultra-wideband (UWB) is defined as a bandwidth greater than 500 MHz or 20% of the arithmetic center frequency. In 2002, the Federal Communications Commission (FCC) has designated 3.1 - 10.6 GHz for unlicensed uses by UWB systems. Along with the frequency band designation, FCC also has set a power spectral density limit for UWB transmitters. UWB technology has a wide application space both in military and in commercial sector. One prominent application is communications, where systems can take advantage of wide bandwidth availability. Signals with a short duration such as a Gaussian monocycle, sinc function, and a fast edge are typically used as transmit waveforms. In order to accommodate the wideband nature of these signals, an antenna that can fully utilize the entire bandwidth is desired for such systems.

Due to its wide band characteristics, UWB systems are susceptible to possible interference from other systems utilizing a subset of or partially overlapping frequency spectrum. Most notably for the UWB, one such example is the IEEE 802.11a band, which spans from 5.15 to 5.825 GHz. A technique to address this issue is to use a notch filter to reject unwanted frequency content. Component filters can be designed in into the system. Alternatively, a notch filter can be integrated into the antenna.

Planar monopole antennas possess qualities that are appealing to UWB communication systems [2]. Wideband matched impedance, omni-directional pattern, compact form factor, and simplistic geometry are such qualities. Recently,

there has been a prolific research work on planar microstrip monopole antennas in the antenna community. The problem of interference and creative methods to provide suppression has received much attention along with the design of the antenna. One general approach is to create an additional resonance on the antenna at the unwanted frequency. Unique variety of shapes and their purposeful placement within the monopole antenna structure that yields secondary resonance have been implemented, providing a notch filter response over a frequency band of interest [3].

In this paper, a novel geometry that provides notch filter characteristics to a planar equiangular spiral antenna (PESA) is presented. As shown in Fig. 1, a secondary resonant structure, in the form of a partial spiral, is implemented on the bottom side of the substrate with via connections to the spirals on the top side. This allows suppression of radiation at the frequency of interest while preserving flat return loss profile outside of the notch band similar to a traditional PESA. The placement and the rejection level of notch band can be readily controlled by two physical parameters. While comparable in size, PESA provides higher directivity and circular polarization option to the planar monopoles.

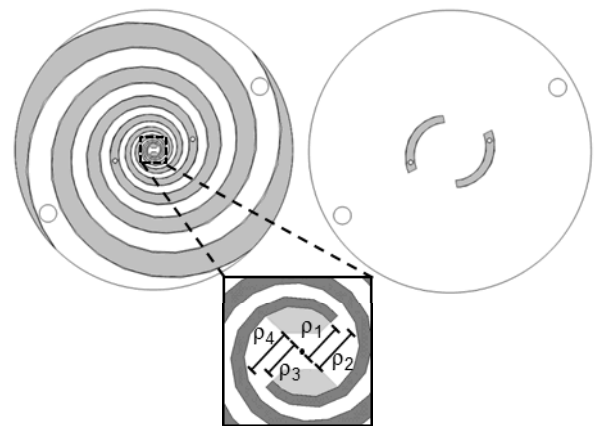


Fig. 1. Dimensional layout of the PESA with the secondary resonant structure: Top side of the substrate (Right), Bottom side of the substrate (Left).

II. ANTENNA DESCRIPTION

A. Equiangular Spiral Antenna

Planar equiangular antennas are completely described by angles. It is this property that gives frequency independent characteristics if the antenna were to expand out to infinity [4].

In practice, PESAs are limited in size, which in turn limits the low end of the operating frequency range. The upper end of the operating frequency range is set by the proximity of the two arms at the feed point. The governing equation for the traditional equiangular spiral curvatures are given below [5], and the corresponding designations for dimensions are depicted in Fig. 1:

$$(1)$$

$$(2)$$

Each arm has a finite width. Equation (2) follows (1) at an angular offset, θ , which determines the width of the arm and in consequence, the spacing between the arms. The variable, a , dictates the expansion rate of the arms. r_0 is the initial radius and n describes the number of turns before reaching the final radius, which determines the size of the overall antenna.

$$(3)$$

$$(4)$$

Equation (3) and (4) are used to create the second arm, which is placed at 180 degrees angular offset from the first arm. In the beginning of the design stage these variable can be set directly, or alternatively can be described with other physical parameter or given specification. Delta is typically set at $\pi/2$ which matches the gap spacing to the width of the arms, naturally fulfilling the self-complementary nature. Upper limit of the desired frequency range sets the initial radius of the antenna. Desired size of the antenna sets the final radius. And the number of turns can be found by realizing that the radiation occurs about one wavelength down the spiral from the feed point. By collating these parameters, the expansion rate can be found using the following equation:

$$\frac{r_f}{r_0} = e^{2\pi n \Delta} \quad (5)$$

The antenna in discussion was designed to cover the FCC's unlicensed UWB band that spans 3.1 GHz to 10.6 GHz. Within this band is the IEEE 802.11a Wi-Fi band that occupies 5.15 to 5.825 GHz. As shown in Fig. 1, on the bottom side of the substrate, a secondary resonant structure to provide a notch filter function for this particular frequency band have been added to the antenna design. It is in a form of a pair of partial spirals that are parallel to the main spirals on the top side. The length and the placement of the spirals determine the bandwidth and center frequency of the notch band. Two vias, one for each arm has been placed at the location where it approximately matches the wavelength of the lower end of the frequency that needs to be tuned out. This is based on the band theory of spiral antennas. Then the partial spirals stem from the vias extending upstream toward the feed point. The two dimensional numbers that control the placement of vias and the length to which it extends can be parameterized to control the placement of the notch band in the operating frequency range.



Fig. 2. A picture of the fabricated antenna with the balun and the support structure.

Overall antenna is circular with a design radius of 3cm. Based on the fact that tapered ends improve the impedance matching performance, region outside of the circular area covered by the radius to the inner edge of the arm has been cut away. Physical radius to the outer edge measures, 24.25 mm. Therefore the actual antenna spans just about 5 mm, as it is evident is Fig. 2. θ is kept at $\pi/2$. The expansion rate is calculated to be 0.135. Inner diameter of the spirals is set to 2 mm. However the feed point gap is tapered toward the center until the gap reaches a 1 cm separation. Spiral makes four turns to extend the lower end of the operating frequency range to the point where the minimum feature size stays above the resolution limit of the PCB plotter used to fabricate the antenna. LDKF's S100 PCB prototyping machine was used for fabrication. With its tools designed for RF applications, machine is capable of realizing 0.2 mm trace and gap width. The minimum feature size for this antenna with the given parameters, is 0.215 mm. The secondary resonant structure is located at 2.11 turns to 2.4 turns with the same trace width as the top side. Rogers RT5880 Duroid substrate at 30 mil thickness is chosen for this design due to its availability.

B. Balun and Mechanical Support

Spiral antennas require a differential input. Consequently, a wideband balun was designed to accompany the antenna. Exponential taper microstrip balun was chosen for its relatively simplistic, and easily parameterizable dimensions [6]. Fig. 3 depicts the balun design. It stretches 35 mm (L_{balun}) by 44 mm (W_{balun}). Same substrate as the antenna was used for balun construction as well. On top side of the substrate is a microstrip line that gradually changes from 50 Ohm width to the width that corresponds to the input impedance of the PESA for this particular substrate. On the bottom side is the ground plane to hold 50 ohm impedance at the feed point for the length that is equivalent to an end-launch SMA connector's ground prongs ($L_{SMA} = 5$ mm, $W_{SMA} = 10$ mm). Then it exponentially tapers to the width that corresponds to the input impedance of the PESA, eventually forming a parallel strip line with the top trace. This allows a gradual change of an unbalanced signal to a balanced signal. The length of the balun is chosen based on

the half wavelength of the lowest operating frequency of the antenna. The size of the substrate outside of the signal traces was chosen based on the formation of the spirals to accommodate screw-hole alignment for mechanical stability.

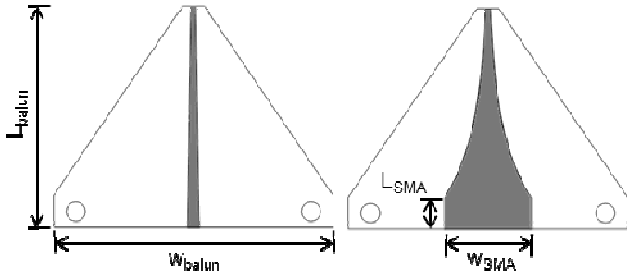


Fig. 3. Dimensional layout of the balun used in conjunction with the PESA: Top side of the substrate (Right), Bottom side of the substrate (Left).

Two 4-40 screw size holes in the spiral and two more on the balun as shown in Fig. 3 have been drilled. L brackets, made out of delrin, are placed over these holes and nylon screws were used to hold them in place.

III. RESULTS AND DISCUSSION

Microwave Studio electromagnetic simulation package by CST was used for simulation. Initially, simulation included the antenna portion only to reduce computation time. Spiral antennas require a balanced feed. A discrete port was used in the middle of the gap between where the spiral arms are the closest. A parametric study on the source impedance revealed that the input impedance of the spiral antenna is approximately around 100 Ohms. For the remainder of the simulation process, the source impedance was set to 100 Ohms. And it was checked regularly through the optimization process that the source impedance was at an optimal value. Number of turns, outer radius, length and location of the secondary structure were parameterized and were tuned until desired response was reached. Then the microstrip balun, which also serves as an impedance transformer was designed to preserve this performance while allowing an unbalanced feed from a 50 Ohm source. All simulation results presented in this paper include the balun in the simulation environment, oriented as shown in Fig. 2.

Fig. 4, shows the impedance matching of the antenna over frequency. Red curve is the return loss profile without the notch filter feature and the blue curve is with the notch filter feature. Spiral antenna without the notch filter has an excellent input impedance matching as expected. VSWR of 2:1 is comfortably met for the entire UWB band. Nearly flat S11 curve above 3 GHz, demonstrates self-complementary nature of the antenna. Also evident in Fig. 4, when the secondary resonant structure is added, mismatch is created at the desired frequency range, covering from 5 to 6 GHz. The peak rejection reaches 12:1 VSWR at 5.5 GHz. The resonant structure does not interfere with frequencies outside of this band as it is evident in the similarity in S11 outside of the notch band.

Fig. 5 compares the VSWR result between simulation and measurement. The blue curve is the measured result. Other than the shift in peak frequency of the notch band, the VSWR curve is quite similar to the simulation result all throughout the

UWB band. This error is fabrication process dependent. The accurate realization of the gap width and the trace is difficult when its size approaches the resolution limit of the machine. Unlike the chemical etching process, where the traces come out as clean strips, but instead they are beveled at the edges. And the spirals are not realized as smooth curves but instead short but visibly straight edges. Also, when removing excess copper, endmill scrapes off the surface of the substrate, making it thinner than intended in the original design.

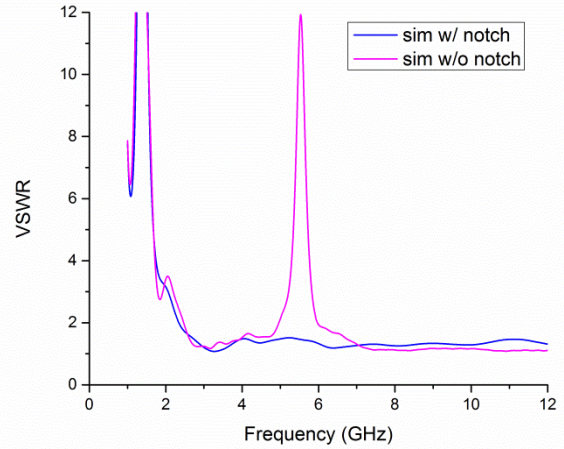


Fig. 4. Simulation result on VSWR comparison for PESA with and without the secondary resonant structure

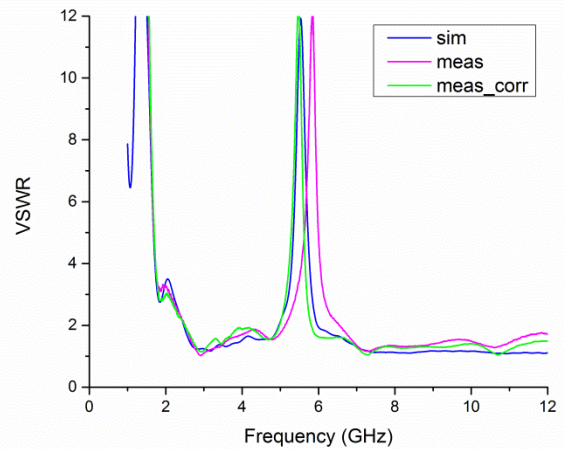


Fig. 5. Comparison of VSWR result between simulation, measured, and measured with process dependent error correction result.

This process dependent shift in frequency can be corrected by iterating through the design and fabrication process one more time, accounting for the observed difference. For this iteration, the peak notch frequency was tuned intentionally lower by the amount equivalent to the error. The end result is the green curve in Fig. 5. The peak clearly is located at the center of the notch band, precisely aligning with the original simulation result.

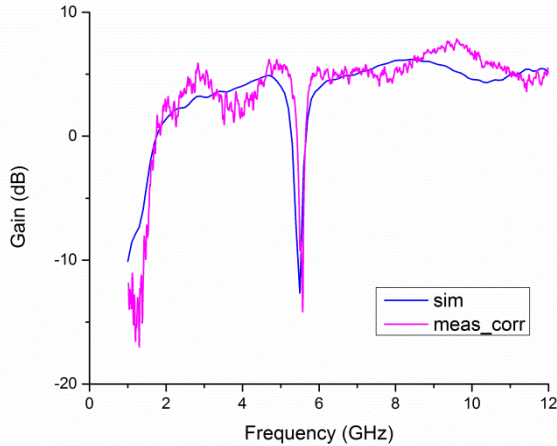


Fig. 6. Far field gain comparison between simulation, and measured with process dependent error correction result.

Gain profile over frequency, depicted in Fig. 6, is obtained from monitoring the far field radiation. The simulation result corresponds to the realized gain, which takes into account the losses at the input. Boresight is chosen for obtaining the data. As expected the gain curve is flat outside of the notch band and within the operating band. But clearly, there is a sharp drop in gain within the notch band. Two antennas, both from the second iteration where the frequency shift error has been accounted for, were set a meter apart inside a partial anechoic chamber. A network analyzer was used to measure the S21 response. Post processing was applied using the Friis transmission equation. The resultant measured gain curve solidly confirms the simulation result. The sharp drop in the gain in both results closely aligns. The slight fluctuation in the measured gain curve at the high end of the frequency range can be attributed to imperfect far-field environment for the test setup.

Observing the current density around the antenna structure at various frequencies reveal the reason for the notch response of the proposed antenna. Fig. 7, depicts current densities at 4 GHz, 5.5 GHz, and 8 GHz, which are below, within, and above the notch band, respectively. The only time when current density around the secondary resonant structure is reaching visibly significant level is when the frequency falls right within the notch band. This observed current explains the reason for strong resonance in the frequency band responsible for notching characteristics.

Fig. 8 shows the radiation pattern for the XY, XZ, and YZ planes according to the coordinate shown in Fig. 7. Frequencies are chosen to follow the same cases as the current density plot. Spiral antennas have a symmetrical radiation pattern about the plane of the antenna. In other words, front to back ratio is ideally unity. Indeed, this property is observed for 4 and 8 GHz. However, for 5.5 GHz, there is a clear difference in the level of radiation suppression between front and back side of the antenna. The main lobe in the outward direction from the bottom side of the board is reduced significantly while the back lobe is suppressed to a lesser degree. This asymmetry is caused by much weaker field cancellation due to

the physical presence of the balun. When the antenna is simulated independently, the symmetrical radiation pattern is observed at 5.5 GHz. For directional applications, RAM can be placed on the side where the balun is present, to purposely reduce the front to back ratio.

If fabrication process resolution can be reduced, the overall dimension of the antenna can be scaled to a smaller form factor while achieving the necessary performance. The original design was approximately 20% smaller but it was scaled up to meet the minimum fabrication limit.

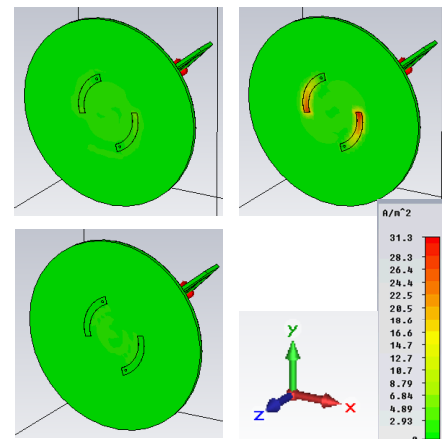
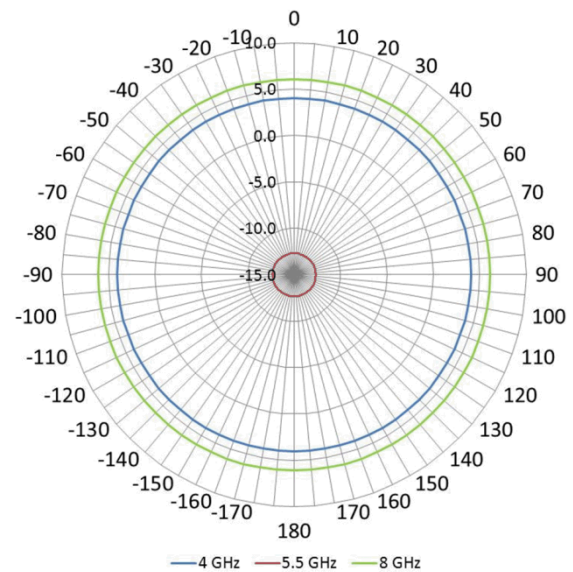


Fig. 7. 3D current density comparison between simulation runs at 4 GHz (Upper Left), 5.5 GHz (Upper Right), 8 GHz (Bottom).



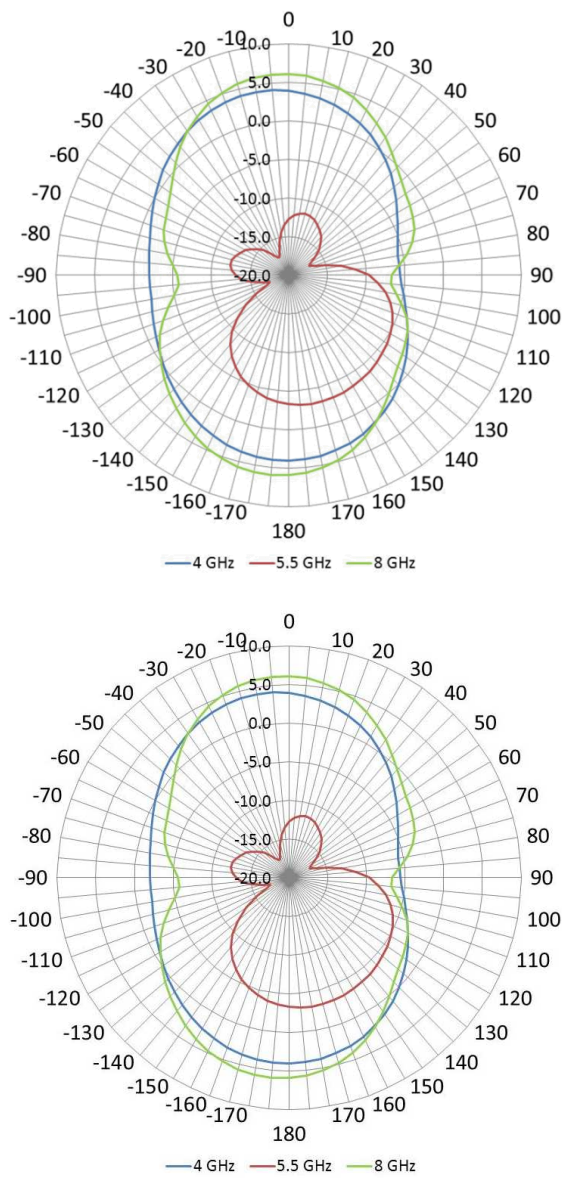


Fig. 8. Radiation pattern from simulation at 4 GHz, 5.5 GHz, and 8 GHz for the XY plane (Top), XZ plane (Center), YZ plane (Bottom) according to the coordinate shown in Fig. 7.

IV. CONCLUSION

A novel planar equiangular spiral antenna for the FCC defined unlicensed UWB band with notch filter characteristics have been presented. By employing a secondary resonant structure at the bottom side of the substrate with parameters to control its location and extension, a notch response in its performance was observed for the 802.11a band. Measured result validated the simulation result, demonstrating that PESA can be a good alternative to planar monopoles with an advantage of having a circular polarization and higher directivity.

ACKNOWLEDGMENT

The authors would like to thank engineers at Lawrence Livermore National Laboratory, Mark Vigars and Jim Zumstein, for their help with fabrication and mechanical work.

This work performed under the auspices of the U.S. Department of Energy by Lawrence Livermore National Laboratory under Contract DE-AC52-07NA27344.

REFERENCES

- [1] Federal Communications Commission, "First report and order in the matter of revision of part 15 of the Commission's Rules Regarding Ultra-Wideband Transmission Systems," ET-Docket 98-153, Apr. 22, 2002.
- [2] L. Jianxin, C. C. Chiau, C. Xiaodong, and C. G. Parini, "Study of a printed circular disc monopole antenna for UWB systems," *Antennas and Propagation, IEEE Transactions on*, vol. 53, pp. 3500-3504, 2005.
- [3] C. Chao-Tang, L. Ting-Ju, and C. Shyh-Jong, "A Band-Notched UWB Monopole Antenna With High Notch-Band-Edge Selectivity," *Antennas and Propagation, IEEE Transactions on*, vol. 60, pp. 4492-4499, 2012.
- [4] V. Rumsey, "A solution to the equiangular spiral antenna problem," *Antennas and Propagation, IRE Transactions on*, vol. 7, pp. 117-117, 1959.
- [5] Dyson, "The equiangular spiral antenna," *Antennas and Propagation, IRE Transactions on*, vol. 7, pp. 181-187, 1959.
- [6] D. M. Pozar, *Microwave Engineering*, 2nd ed. New York, NY: Wiley, 1998, ch. 5.